Published in final edited form as:
Chem Soc Rev. 2018 May 21; 47(10): 3406–3420. doi:10.1039/c7cs00827a.

Minimalistic peptide supramolecular co-assembly: expanding the conformational space for nanotechnology

Pandeeswar Makam[ID,a] and **Ehud Gazit**[ID,*,a,b]

[a]Department of Molecular Microbiology and Biotechnology, George S. Wise Faculty of Life Sciences, Tel Aviv University, Tel Aviv 6997801, Israel

[b]Department of Materials Science and Engineering, Iby and Aladar Fleischman Faculty of Engineering, Tel Aviv University, Tel Aviv 6997801, Israel

Abstract

Molecular self-assembly is a ubiquitous process in nature and central to bottom-up nanotechnology. In particular, the organization of peptide building blocks into ordered supramolecular structures has gained much interest due to the unique properties of the products, including biocompatibility, chemical and structural diversity, robustness and ease of large-scale synthesis. In addition, peptides, as short as dipeptides, contain all the molecular information needed to spontaneously form well-ordered structures at both the nano- and the micro-scale. Therefore, peptide supramolecular assembly has been effectively utilized to produce novel materials with tailored properties for various applications in the fields of material science, engineering, medicine, and biology. To further expand the conformational space of peptide assemblies in terms of structural and functional complexity, multicomponent (two or more) peptide supramolecular co-assembly has recently evolved as a promising extended approach, similar to the structural diversity of natural sequence-defined biopolymers (proteins) as well as of synthetic covalent co-polymers. The use of this methodology was recently demonstrated in various applications, such as nanostructure physical dimension control, the creation of non-canonical complex topologies, mechanical strength modulation, the design of light harvesting soft materials, fabrication of electrically conducting devices, induced fluorescence, enzymatic catalysis and tissue engineering. In light of these significant advancements in the field of peptide supramolecular co-assembly in the last few years, in this tutorial review, we provide an updated overview and future prospects of this emerging subject.

1 Introduction

Supramolecular chemistry, also known as “chemistry beyond the molecule”, is a bottom-up approach to fabricate well-ordered architectures and exists in nature at various scales.1,2 This method mainly deals with the rational design of minimalistic molecular building blocks

Pandeeswar Makam: http://orcid.org/0000-0003-1114-8089
Ehud Gazit: http://orcid.org/0000-0001-5764-1720
ehudg@post.tau.ac.il.

Conflicts of interest
There are no conflicts to declare.

Europe PMC Funders Author Manuscripts

that undergo a spontaneous predefined self-assembly process *via* specific, directional, tunable and reversible, non-covalent interactions such as electrostatic forces, hydrogen bonding, aromatic π–π stacking, metal chelation and van der Waals interactions. The most intriguing aspect of supramolecular assemblies is the dynamic nature of the non-covalent bonds; this makes them produce nanostructures with adaptable, self-healing and stimuli-responsive properties.3 Moreover, supramolecular interactions are the basis for the structure and function of all living systems.4 There are numerous examples with simple to complex supramolecular assemblies in biological systems including the formation of cell membranes from simple hydrophobic interactions among amphiphilic phospholipid molecules, DNA double helix formation through specific hydrogen bonding interactions between the nucleobases, and the complex protein folding into a precise tertiary and quaternary structure from a polypeptide chain. Using nature as a source of inspiration, many synthetic supramolecular nanomaterials have been created by iterative interaction among the rationally designed small molecular building blocks, by specific non-covalent folding of macromolecules (*e.g.* foldamers), or by the combination of both.4

The naturally occurring and robust self-associated amyloid fibril assemblies encouraged the exploitation of peptides as biomimetic supramolecular structural motifs in nanotechnology.5 Over the years, peptides have been proved to be excellent structural units for the creation of more complex supramolecular architectures and functions.5–11 In contrast to other structural building blocks, peptides possess many unique and desirable features for biotechnology applications, to name a few, biocompatibility, sequence-specific secondary structures, chemical diversity, biomolecular recognition and ease of synthesis.12,13 Furthermore, peptide supramolecular assemblies exhibit rich diversity in nano- and microstructures, including hydrogels, fibers, tubes, rods, films, plates, nanocages, vesicles *etc.* The dynamic nature of peptide assemblies allows spatial and temporal control over the end-product architectures.14 In addition, control over peptide supramolecular organization was achieved by the application of external stimuli, such as pH, temperature, chemicals, enzymes, solvents, magnetic and electric fields. These stimuli further uniquely serve to alter the properties and characteristics of peptide nano-assemblies. Moreover, peptide assemblies show diverse physicochemical properties and are therefore explored for various material science and biological applications, such as energy storage devices, displays and light-emitting devices, ferroelectric and piezoelectric components, super-hydrophobic surfaces for self-cleaning applications, composite reinforcement, scaffolds for inorganic ultra-structures, metal–organic frameworks, ultra-sensitive sensors, 3D hydrogel scaffolds for tissue engineering, drug delivery and many more.6,10,12,15–17

Despite the advances in the fabrication of remarkable functional nanomaterials, the use of unimolecular peptide self-assembly processes has been limited by a lack of chemical diversity and functional complexity. In this context proteins in biological systems exhibit rich physiochemical diversity *via* copolymerization of 20 different precisely positioned amino acids which are essential for the various important functions of life. Similarly, supramolecular co-assembly between two or more distinct functional peptide building blocks results in nanostructures of wide structural complexity and chemical diversity. The intriguing noncovalent interactions within the supramolecular co-assembly make them simple and avoid complicated synthesis, purification, processing and recycling steps as

compared to covalent co-polymers. The incorporation of different building blocks synergistically combines their properties, thereby facilitating multiple tasks from a co-assemble system, which are not possible from a single component self-assembly process. Moreover, the interplay between the mixing ratio of the individual building blocks allows the adaptable co-assembly mechanism to tune the morphology and the resulting physical, chemical and mechanical properties. These unique characteristics have attracted researchers to explore the scope of peptide supramolecular co-assembly to further extend the conformation space of peptide nanotechnology. Herein, we review the recent progress in the design principles of minimalistic peptide supramolecular co-assembly and the relevant applications of this new class of bio-inspired multifunctional supramolecular architectures.

Unlike peptide self-assembly of the same motif (red or blue bricks in Fig. 1), supramolecular co-assembly involves the combination of two or more peptide building blocks (red and blue bricks) together to form an ordered organization.15 Similar to copolymer chemistry paradigms, the co-assembly process can take place in four possible ways, namely cooperative co-assembly, orthogonal co-assembly (self-sorting), random co-assembly and destructive co-assembly.18 In cooperative co-assembly, the two peptide building blocks interact with each other to yield architectures containing both components arranged in an alternating fashion. Cooperative peptide co-assembly can be achieved by mixing two very similar peptides, which are only slightly different in structure. Using this methodology, one can design the incorporation of different types of peptides within the co-assembled structure to induce multi-functionality and to achieve supramolecular charge transfer mixed stack structures between donor and acceptor molecules for optoelectronic applications.19,20 In contrast, orthogonal (self-sorted) co-assembly comprises peptide building blocks assembled independently while in the presence of each another. This kind of assembly allows the formation of various architectures, such as interpenetrating networks of bulk heterojunctions containing domains or layers of one of the individual components. This phase separated hybrid co-assembly is potentially desirable in the development of p–n heterojunction photovoltaics. Designing orthogonal co-assembly is quite challenging, however, as very different non-covalently binding motifs (in terms of the extent of self-assembly, strength, type *etc.*) tend to show a thermodynamic preference for self-sorting. Co-assembly of the two peptides can also be somewhere between these two extremes with varying degrees of mixing and self-sorting. Random co-assembly refers to the organization of the peptide building blocks without any precise order. On the other hand, co-assembly of two distinct peptides may take place in a destructive manner, resulting in disruptive co-assembly, where one building block acts as a stopper for the assembly of the other. This assembly is very useful in controlling the physical characteristics of the resultant architectures.21

2 Peptide co-assembly strategies

2.1 Aromatic interactions

In order to promote co-assembly, Nilson *et al.* exploited the complementary quadrupole effects between Fmoc-phenylalanine (Fmoc-F, **1**) and Fmoc-mono and penta halogenated-phenylalanine (**2**) (Table 1).22 The aromatic side-chain groups (benzyl and pentahalo benzyl) possess complementary quadrupole electronics and therefore exhibit attractive face-

to-face quadrupole stacking interactions. The equimolar mixtures of Fmoc-F and Fmoc-pentafluorobenzyl-phenylalanine (Fmoc-PFB-F) readily co-assembled into two-component high aspect ratio 1D fibrils and hydrogels. However, under similar conditions, the individual components, **1** or **2**, failed to exhibit hydrogelation. Furthermore, the co-assembly of Fmoc-F with equimolar mixtures of monohalogenated (F, Cl, and Br) Fmoc-F derivatives was also found to form two-component co-assembled fibrils. Collectively, the results suggest that the complementary face-to-face quadrupole stacking interactions on the peptide backbone promote co-fibrillization mediated by subtler π–π effects arising from the halogenation of the benzyl side chain.

Adopting a similar strategy, Lin *et al.* described the co-assembly of pentafluorobenzyl-phenylalanine (PFB-F, **3**) and pentafluorobenzyl-diphenylalanine (PFB-FF, **4**) under physiological pH conditions.23 The equimolar mixture of **3** and **4** was found to co-assemble into a self-supporting hydrogel embedded within a nanofibers network. The detailed spectroscopic characterization of the blend gel revealed that complementary quadrupole aromatic stacking along with intermolecular hydrogen-bonding interactions were the major driving forces behind the co-assembly. Furthermore, the biocompatibility of this co-assembled hydrogel was confirmed by survival ratio experiments using CTX TNA2 and MCF-7 cells.

Very recently, Adler-Abramovich *et al.* explored co-assembly between Fmoc-FF (**5**) and Fmoc-PFB-F (**6**) and its synergistic effect on the mechanical properties of the resulting hybrid hydrogels.24 Interestingly, the equimolar mixture of Fmoc-PFB-F and Fmoc-FF resulted in the formation of an ultra-rigid hybrid hydrogel with remarkable mechanical properties. The storage modulus (G') was found to be as high as 190 kPa, an order of magnitude higher than that of the hydrogels self-assembled by each individual component alone. Moreover, the mechanical properties of the supramolecular co-assembled hybrid hydrogels could be easily controlled by changing the molar ratios of the individual building blocks.

The impact of intermolecular peptide hydrogen bonding and aromatic interactions on supramolecular co-assembly was investigated by Ulijn *et al.* with two distinct types of designed peptide amphiphiles.18 The studied system consists of pyrene (Py) conjugated peptide amphiphiles (Py-YL (**7**), Py-S (**8**)) and their analogous 9-fluorenylmethoxycarbonyl (Fmoc)-capped peptides (Fmoc-YL (**9**) and Fmoc-S (**10**)). These peptides possess distinct self-assembly abilities; the Fmoc-YL and Py-YL form hydrogels *via* aromatic and β-sheet type H-bonding interactions, whereas the self-assembly of surfactant type **8** and **10** is solely governed by aromatic stacking and hydrophobic or hydrophilic interactions. Remarkably, three supramolecular co-assembly modes (cooperative, disruptive and orthogonal) were achieved by mixing a different combination of individual peptide constituents. The detailed spectroscopy results suggested that the mode of co-assembly was adopted based on the nature of the individual building blocks. The combination of two structurally different peptide components (Py-YL/Fmoc-S and Fmoc-YL/Py-S) results in orthogonal co-assembly. On the other hand, structurally similar peptides (Py-YL/Fmoc-YL and Py-S/Fmoc-S) followed the cooperative co-assembly process. In addition, the disruptive co-assembly pathway was proposed to take place with peptides of similar aromatic moiety but differing in

their ability to form β-sheet type H-bonding interactions (Py-YL/Py-S) and (Fmoc-YL/Fmoc-S). Hence, for the first time, this study provided new insights into the design rules for making different kinds of co-assembly structures based on aromatic peptide amphiphiles.

2.2 Electrostatic interactions

To explore the noncovalent electrostatic attractive interactions in co-assembly design, Lynn *et al.* studied two similar positively and negatively charged peptides (Ac-KLVFFAL-NH_2 (**11**) and Ac-(pY) LVFFAL-NH_2) (**12**) differing only in their N-terminal residues, lysine and phosphotyrosine (pY), respectively.25 The individual peptides were self-assembled into cross-β bilayer membrane leaflets of nanotubes with charged inner and outer surfaces. Co-assembly of these oppositely charged peptides resulted in interesting cross-β bilayer nanotubes with dense negative external and positive internal solvent exposed surfaces containing both homogeneous and heterogeneous leaflet interfaces. Furthermore, the distinct organization showed unique properties and a controllable rate of the co-assembly process. Moreover, they could control the asymmetry across the peptide bilayer and along the lateral axis of the nanotube membranes.

Furthermore, Stupp and co-workers described the co-assembly between a fluorescent peptide amphiphile that is covalently conjugated with a stilbene chromophore and a shorter non-fluorescent peptide amphiphile of complementary charge.26 The β-sheet mediated co-assemblies displayed tunable molar ratio dependent fluorescence with high quantum yield and supramolecular chiral induction to the achiral segment of the fluorescent peptide amphiphile. Furthermore, they exhibited a fluorescence resonance energy transfer process in the presence of a fluoresceintagged heparin acceptor. Next, they investigated the co-assembly behavior of a new class of peptide amphiphiles having opposite peptide sequence polarity (**13** and **14**, Table 1).27 When mixed, these designed peptides with free N- and C-termini co-assembled into β-sheet secondary structures to produce highly thermally stable nanofibers. Remarkably, these structures were found to be more stable than the co-assemblies between the peptide amphiphiles of identical polarities. Furthermore, the co-assemblies containing free N-termini on the surface of the nanofibers were able to bind the growth factors bone morphogenetic protein-2 (BMP-2) and transforming growth factor β1 (TGF-β), which are important in stem cell differentiation. Following similar oppositely charged peptide amphiphilic design principles, Guler and co-workers demonstrated supramolecular co-assembled nanofibers for drug delivery and tissue engineering applications.33,34

2.3 Enantiomeric interactions

Chirality is one of the unique features of amino acids. This fascinating stereochemical information was utilized by Schneider *et al.* and they revealed chirality effects as a new design modality to control the mechanical properties of hydrogels formed from co-assembling peptide enantiomers.29,35 Two enantiomeric β-hairpin self-folding peptides **15** and **16** (Table 1) were designed and allowed to co-assemble in their equimolar mixtures to form racemic hydrogels. Remarkably, the co-assembled racemic β-hairpin fibrillar hydrogels exhibited a 4-fold higher rigidity compared to enantiomerically pure gels formed by either peptide alone. This mechanical enhancement is attributed to the synergetic effect of co-

operative co-assembly driven hydrophobic interactions between enantiomers which are not present in enantiomerically pure fibrils.

In a similar attempt, Nilsson *et al.* developed amyloidinspired rippled β-sheet fibrils by the co-assembly of L-(**17**) and D- (**18**) enantiomeric Ac-$(FKFE)_2$-NH_2 amphipathic peptides.28 The designed enantiomeric peptides displayed a higher tendency to co-assemble into alternating L- and D-peptides in a "rippled β-sheet" orientation rather than into the self-sorted β-sheet assembly attributed to enthalpic advantage. Moreover, the recemic co-assembled structures were resistant to proteolytic degradation,36 unlike the individual pleated β-sheet fibrils of self-assembled L-peptides, which are readily degraded by common proteases.

2.4 External stimuli induced peptide co-assembly

Recent advancements have demonstrated the regulation of peptide co-assembly behavior by external stimuli. This approach is emerging as a more powerful tool to control the order of co-assembly by a predictable 'molecular trigger' and thus allows complex structures to be designed in a targeted manner. In this context, Adams *et al.* designed naphthalene-functionalized dipeptide hydrogelators **19** and **20** (Table 1).30 These molecules start self-assembling following a decrease in the solution pH from 10.5 to just below the apparent pK_a of the terminal carboxylic acid. The overall hydrophobicity of the molecule determines the apparent pK_a of the peptide. Therefore, the pH at which each peptide begins to self-assemble can be precisely controlled and predictable. Here, the authors coupled the predictable apparent pK_a of the designed peptide molecules with the slow hydrolysis of glucono-δ-lactone (GdL) to gluconic to allow orthogonal co-assembly. These *in situ* pH-triggered assemblies allowed the rate of self-sorting between the co-assembled peptides to be predefined and tunable.

The same concept was further extended to electrochemically trigger self-sorted peptide co-assembly between dipeptides **21** and **20** (Table 1).31 Here, a pH gradient was generated electrochemically by adding hydroquinone (HQ) into the peptide solution. Application of a current to the working electrode resulted in the oxidation of HQ and the simultaneous release of protons. As a result, a localized pH drop at the electrode surface could be produced, which was controllable by modulating the rate of formation of protons at the electrode surface and the diffusion coefficient of the free protons in the solution. This method allowed *in situ* control over the spatial and temporal organisation and composition of the multicomponent co-assembly.

2.5 Enzyme driven co-assembly

Ulijn *et al.* described supramolecular minimalistic peptide gelator/surfactant co-assembly that can be triggered by a biocatalytic action.32 The designed peptide systems are composed of phosphatase responsive phosphorylated Fmoc-FYp (**22**) pre-gelator and a surfactant-like amino acid (or peptide), Fmoc-X [X = S (**24**), T (**25**) or RGD (**26**)]. The mixture of Fmoc-FYp and Fmoc-X in the presence of dephosphorylation enzyme (alkaline phosphatase) demonstrated the transformation of the morphology from micellar structures to fibers and became a hydrogel. Interestingly, the surface of the co-assembled fibers is decorated with surfactant functionalities. Furthermore, the gelation kinetics and resultant properties such as

gel stiffness and supramolecular organization of the building blocks were found to be adaptable by varying the enzyme concentration.

3 Applications of peptide co-assembly

3.1 Nanostructure physical dimension control

Among the numerous self-assembling peptide sequences explored so far, a specifically aromatic short dipeptide building block, diphenylalanine (FF, **27**), the core recognition motif of Alzheimer's disease β-amyloid polypeptide, has emerged as one of the smallest and most widely studied self-assembling peptides.12 In aqueous medium, FF can spontaneously self-assemble into robust nanotubes *via* noncovalent interpenetrated zipper-like aromatic interlocks and hydrogen bonding interactions. These FF nanotubes exhibit unique properties, containing photoluminescence, optical waveguiding, semiconductivity and Ferro-, piezo- and thermoelectrical responses.5 However, the inherent sequential self-assembly mechanism of FF in solution results in the formation of nanotubes with a wide range of size distributions. In order to control the physical dimensions of the peptide nanotubes, a supramolecular co-assembly strategy was utilized. We introduced the FF dipeptide along with its analog *N*-(*tert*-butoxycarbonyl)-L-F-L-F-COOH (Boc-FF (**28**)) to allow their co-assembly (Fig. 2).21,37 In line with the covalent copolymer phenomenon, the Boc-FF acts as a blocker to the self-assembly of FF and, at a particular ratio, results in the desired length scale of the co-assembled peptide nanotubes (Fig. 2B). The nature of this disruptive co-assembly was determined by demonstrating the bimolecular composition of the formed nanotubes using mass spectrometry (Fig. 2D). The controlled length distribution of the nanotubes at different molar ratios of Boc-FF to FF was confirmed by electron microscopy and shown to fit a fragmentation kinetics model (Fig. 2C). Therefore, this approach enabled us to control the self-assembly process by regulating the elongation and length distribution of FF tubular structures. Furthermore, the combination of two types of building blocks in the same nanometric architecture gave rise to more complex architectures with extended physical properties. More importantly, this method is solution processable and therefore, could be adaptable to integrate into large area flexible device applications.

3.2 Creation of new non-canonical complex topologies

Aiming to create complex architectures from simple aromatic dipeptides, Reches *et al.* adapted the co-assembly technique using FF (**27**) and its Boc protected analog (Boc-FF, **28**) (Fig. 3A).38 Individually, FF forms tubular structures while its Boc protected analog self-assembles into spherical aggregates. Blending them together in 50% ethanolic HFIP solution resulted in a new morphology resembling beaded strings, where the spherical structures are threaded on top of the elongated assemblies, thus designating these assemblies as "biomolecular necklaces". In addition, dilution and re-concentration experiments indicated the reversibility of the co-assembly process. Furthermore, the co-assembled "biomolecular necklaces" showed significant stability over time and heating–cooling cycles, but disassembled upon exposure to strong acid or base. The possible mechanism of co-assembled "biomolecular necklace" formation was further proposed based on the necklace model of polyelectrolyte chains, where the counterion condensation on the backbone of the polyelectrolyte results in a necklace-like structure. A similar effect can be seen in the co-

assembly of negatively charged Boc-FF and zwitterionic FF. The aromatic interactions among the peptide monomers lead to the formation of a sequence of negatively charged units which consequently behaves as a polyelectrolyte chain. In order to minimize its free energy, this polyelectrolyte peptide chain further collapses into a condensed spherical globule.

A later study demonstrated co-assembly of FF (**27**) and Fmoc-(L)DOPA(acetonated)-(D)F-OMe (**29**) into a fine-tuneable variety of globular assemblies (Fig. 3B).39 Under the studied experimental conditions, the individual peptides self-assembled into spherical aggregates. Interestingly, mixing of these two peptides resulted in new types of concentration-dependent co-assembled morphologies. The low equimolar peptide concentrations (1 mg mL^{-1} each) generated oval biconcave disk-shaped nanostructures, similar to the morphology of red blood cells (RBCs). However, at higher concentrations (2 mg mL^{-1} each) the peptides co-assembled into spherical nanostructures with bulges on the outer surface, similar to the morphology of white blood cells. However, a 2 : 1 Fmoc-(L)DOPA(acetonated)-(D)F-OMe to FF ratio generated disk shared nano-assemblies. In addition, the combination of Fmoc-(L)DOPA(acetonated)-(D)F-OMe with other FF analogs (*i.e.*, Boc-FF-COOH and Fmoc-FF-COOH) resulted in spherical assemblies. Furthermore, the RBC-like co-assembled structures demonstrated adsorption of an anticancer drug (doxorubicin) with sustainable drug release kinetics.

Recently, Wei and co-workers explored the co-assembly of FF (**27**) and FFF (**30**) peptides at various mass ratios using molecular dynamics simulations followed by experimental validation (Fig. 3C).40 The extensive simulation studies revealed that mixing FF and FFF at different ratios resulted in diverse co-assembled ordered nanostructures, including both canonical geometries (hollow nanotubes and spherical nanovesicles, and solid nanorods and nanospheres) and non-canonical topologies, such as toroid-like nanostructures. Remarkably, the toroid morphology is only observed in the co-assembly of FF and FFF, and the topology and geometry of this assembly are very much distinct from the extensively studied individual self-assembly structures of FF and FFF alone. The unique toroid nanostructures were often observed in the co-assembly mixture when the mass percentage of the FFF peptide (P_{FFF}) ranged between 0.167 and 0.33. Systemic co-assembly simulations as a function of P_{FFF} ratios demonstrated the ratio-dependent discontinuous nanostructure morphology transition from hollow to solid assemblies. With the increase of the P_{FFF} ratio, a decrease in hallow structures and an increase of solid assemblies were identified, while the toroid structures appeared to be an intermediate morphology between these structural transformations. The thorough analysis indicates that the FFF peptide has a larger bulky hydrophobic side chain compared to the FF peptide and therefore its side chains are buried more closely to protect from water exposure. Hence, in the low P_{FFF} mixture, the closely packed FFF favors negative curvature, resulting in a hollow nanostructure. The gradual increase of P_{FFF} in the FFF–FF mixture decreases the peptide–water interactions, thereby shifting the conformations toward less water accessible solid architecture. The intermediate toroid structure formation is determined by the extent of competition between the FF–water and FFF–water interactions within the FFF–FF mixture. Thus, the creation and regulation of new co-assembled geometries can be easily controlled by modulating the FFF : FF mass ratio.

Another very promising approach was described by Xu *et al.* wherein aromatic–aromatic interaction driven co-assembly can be utilized to mimic the conformational restriction of peptides in a protein (Fig. 4).41 The well-known β-sheet motif (RMLRFIQEVN) of an irisin protein was fragmented into two complementary pentapeptides and their C-terminals were conjugated with an aromatic pyrene motif (RMLRF-Py (**31**) and IQEVN-Py (**32**)). The designed peptide conjugates were capable of forming stable co-assemblies *via* pyrene aromatic–aromatic interactions and seven intermolecular hydrogen bonds between the complementary peptide sequences. In line with the design strategy, the simple mixing of complementary peptide conjugates results in a self-supported supramolecular hydrogel. Transmission electron microscopy demonstrated the formation of a uniform width high aspect ratio nanofibrilar network, while under similar conditions, the individual peptide conjugates fail to form hydrogels, suggesting co-assembly driven hydrogelation. Furthermore, a detailed spectroscopic investigation revealed that a secondary structural transformation from α-helix to β-sheet conformation drove the co-assembly of the complementary peptide conjugates. This report thus illustrates a novel bioinspired approach to control molecular recognition and to generate supramolecular peptide nanofibers with predefined secondary structures in water by rationally using protein structures as the blueprint.

3.3 Light-harvesting systems

MacPhee *et al.* used the peptide co-assembly strategy as a simple and efficient route to transfer energy between donor and acceptor chromophores for the creation of light-harvesting system (Fig. 5).42 A known short peptide (YTIAALLSPYS) that spontaneously self-assembles into a β-sheet multimolecular fibrillar morphology was chosen to be functionalized at the N-terminus with luminescent donor and acceptor moieties. The donor-peptide constituent was constructed by conjugating the long lifetime excited-state transition-metal complex bis(2,2′-bipyridine)-4′-methylcarboxybipyridineruthenium with a flexible aminohexanoic acid linker (**33**). Similarly, the acceptor peptide conjugate was designed with Alexa 647 (**34**). Thus, the strong β-sheet forming peptide allowed the ordered co-assembly of the two non-assembling fluorophores. The close proximity between the donor–acceptor peptide conjugates within the quasi-one-dimensional fibrillar architecture promoted resonance energy transfer. Indeed, the excitation of the co-assembled nanofibers (50% (v/v) acetonitrile (MeCN)/water solution) at the donor absorption maximum (λ_{ex} = 465 nm) showed a significant acceptor emission (λ_{em} ~ 660 nm). This effect exemplified the rapid excitation energy transfer from the numerous donor species to spatially defined acceptor groups, similar to the natural light harvesting process in plants.

In the same way, Adams *et al.* reported an energy transfer process in co-assembled dipeptide hydrogels.43 At low pH (controlled by hydrolysis of GdL), the naphthalene-FF (**35**) self-assembled into a fibrous hydrogel network *via* β-sheet formation between the peptide segments and the aromatic π–π stacking interactions of the naphthalene groups. This was experimentally corroborated by fluorescence emission shoulder bands at 370 nm attributed to the π-stacked naphthalene moieties. To induce an energy transfer process, the acceptor chromophores (dansyl (**36**) or anthracene derivative), which have absorption maxima at 350–370 nm, were co-assembled with naphthalene dipeptide without disturbing its hydrogelation.

This co-assembly strategy exhibited successful energy transfer by displaying a decrease in the fluorescence emission of naphthalene (at 355 nm), accompanied by an increase in the acceptor's emission band (485 nm). Moreover, this co-assembly driven light harvesting process can be controlled by the overall pH of the solution *via* GdL hydrolysis kinetics.

Later, Tovar *et al.* demonstrated energy transport in two-component co-assembled nanostructures composed of π-conjugated peptides containing oligo-(*p*-phenylenevinylene)-based donor units (**37**) and quaterthiophene-based acceptor units (**38**) in completely aqueous environments.44 The β-sheet forming peptide (DFAA) organized the central π-conjugated donor–acceptors into a 1D mixed stack geometry, thus promoting energy migration along the stacking direction. Detailed steady-state and time-resolved photophysical measurements further validated the energy transport process within the co-assembled nano-structures. The fluorescence spectra recorded following excitation at the donor absorption maxima displayed significant fluorescence emission quenching of the donor unit, accompanied by an increase in acceptor emission. Interestingly, these spectral changes were observed even at very low concentrations of acceptor peptide conjugate fraction (1 mol%), signifying the funnel-like energy transduction mechanism. Furthermore, the modulation of the co-assembly process *via* pH and temperature and the associated tunable energy migration process was demonstrated. Further recent developments conducted by Tovar, Adams, and co-workers showed the pH programmable kinetically controlled co-assembly process (mixed stack to self-sorted or *vice versa*) of multichromophoric peptide hydrogels and its impacts on the energy transfer process between the donor–acceptor conjugated peptides.45

3.4 Conducting architectures

In order to enhance the electrical transport properties, Guler and co-workers described the supramolecular co-assembly strategy between n-type (π-electron acceptor) and p-type (π-electron donor) π-conjugated complementary peptide amphiphiles in aqueous media (Fig. 6).46 A well-studied n-type naphthalene diimide (NDI, π-acidic with molecular quadrupole moment Q_{zz} = +18.6 B) was functionalized to a β-sheet forming hexapeptide sequence (H_2N-Ahx-VVAGEE-Am) to obtain an n-type peptide amphiphile (**40**) bearing a negatively charged end group. Similarly, the complementary p-type pyrene (π-basic, Q_{zz} = −13.8 B) was conjugated to the positively charged β-sheet forming hexapeptide sequence (H_2N-Ahx-VVAGKK-Am), producing a p-type peptide amphiphile (**39**). In aqueous medium, both peptide amphiphiles separately self-assembled into high aspect ratio fibrils with a uniform diameter of 11 ± 1 nm. However, mixing these two-transparent complementary peptide amphiphiles at a 1 : 1 ratio under similar conditions resulted in a pink color solution, indicating the formation of alternative π-electron donor–acceptor charge-transfer (CT) complexation. The detailed spectroscopic and microscopic co-assembly investigations revealed the presence of one-dimensional nanowires consisting of highly ordered alternately mixed stack n/p domains supported by non-covalent CT, hydrogen bonding and electrostatic interactions. The maximum overlap of $LUMO_{NDI}$ with $HOMO_{pyrene}$ within the CT n/p nanowires explained the strong association constant (K_A) of 5.18×10^{-5} between the co-assembled peptide amphiphiles. Moreover, the electrical measurements on these co-assembled n/p nanowire films were estimated to be 1.65×10^{-5} S cm^{-1} (Fig. 6C), which is 2400 times more conductive than the individual n-type peptide film (7.6×10^{-9} S cm^{-1}) and

10 times more than that of the p-type film (1.97×10^{-6} S cm^{-1}). The significant enhancement in conductivity in the n/p co-assembly was attributed to the strong intermolecular charge-transfer interactions between the pyrene and NDI peptide conjugates.

Furthermore, ordered n/p orthogonal co-assembled nanomaterials were constructed by Carrascosa, Martin and co-workers.47 The p-type **π**-extended tetrathiafulvalene (TTF) donor was conjugated to a pentapeptide sequence (H_2N-AGAGA-COOH) with a carboxylic acid in the termini position (**41**). The complementary n-type acceptor perylene-bisimide (PBI) was symmetrically functionalized with polar tails carrying guanidinium (**42**) or quaternary ammonium groups (**43**) in the terminal positions. Initially, the p-type peptide conjugate and n-type PBI were self-organized separately, thereby obtaining n- and p-nanofibers at the same scale with complementary surface charges. The electrostatic interaction driven co-assembly of the two complementary self-assembling nanofibers gave rise to alternately segregated n/p nano-domains. More interestingly, these n/p-co-assembled heterojunctions showed remarkable photoconductivity values of up to 0.8 cm^2 V^{-1} s^{-1} (Fig. 6D).

Ulijn and co-workers demonstrated the non-aqueous self-assembly of p-type tetrathiafulvalene (TTF)-conjugated FF and LLL amide derivatives (TTF-FF-NH_2, **44** and TTF-LLL-OMe (**45**)) into one-dimensional nanofibrous self-supporting gels.48 These gels were successfully doped with complementary n-type acceptors such as 7,7,8,8-tetracyanoquinodimethane (TCNQ, **46**) and iodine vapor to form stable co-assembled charge transfer gels. The current–voltage (*I*–*V*) measurements on this xerogel nanofiber network displayed a remarkable enhancement in the conductivity values from 1.9×10^{-10} S cm^{-1} (undoped) to 3.6×10^{-4} S cm^{-1} when co-assembled with TCNQ and 6.4×10^{-7} S cm^{-1} when exposed to iodine vapor (Fig. 6E).

3.5 Biocatalytic assembly

Liu, Luo and co-workers constructed a hydrolase model *via* supramolecular co-assembly of two similar short peptides (Fmoc-FFH-$CONH_2$ (**47**) and Fmoc-FFR-$CONH_2$ (**48**)) amphiphiles (Fig. 7).49 In aqueous medium, the Fmoc-FFH-$CONH_2$ self-assembled into self-supported hydrogels composed of uniform, high aspect ratio cylindrical nanostructures several micrometers in length and about 10 nm in diameter. The polar imidazolyl groups on the surface of these nanotubes acted as catalytic centers, exhibiting catalytic activity for *p*-nitrophenyl acetate (*p*-NPA) hydrolysis. In order to stabilize the transition state of the hydrolytic reaction, the surface of the Fmoc-FFH-$CONH_2$ nanotubes was decorated with guanidyl groups *via* co-assembly with Fmoc-FFR-$CONH_2$. At a suitable molar ratio of Fmoc-FFH-$CONH_2$: Fmoc-FFR-$CONH_2$ (20 : 1), the co-assembled nanostructures exhibited a remarkable 519-fold higher catalytic efficiency as compared to a control reaction without the catalyst (Fig. 7C). The significant improvement in the hydrolase activity was mainly attributed to the synergy of the reasonable distribution of binding sites (hydrophobic interior), transition state stabilization (guanidyl groups) and catalytic centers (imidazolyl groups) within the co-assembled peptide nanotubes (Fig. 7B). Furthermore, this novel artificial co-assembled peptide hydrolase model is biocompatible and therefore appears to be

a promising minimalistic artificial hydrolase model to treat inflammation, anorexia, edema and other diseases.

A similar supramolecular co-assembled peptide artificial hydrolase was developed by Qi and co-workers by combining catalytic triads (Fmoc-FFH, Fmoc-FFS, and Fmoc-FFD) with Fmoc-FF.50 In addition, to enhance the hydrolysis activity and selectivity, a unique molecular imprinting method was applied. The *p*-NPA was used as a molecular template to pre-organize the catalytic triad residues into the appropriate orientation, which was further fixed through the supramolecular nanostructure formation. Consequently, the removal of the template resulted in a higher exposure of the catalytic triad residues at the catalytic center, thereby increasing the efficiency of the artificial co-assembled enzyme (7.86 times higher than nonimprinted co-assembled triads and 13.48 times higher than self-assembled Fmoc-FFH), as well as its selectivity towards the imprinted substrate (*p*-NPA).

3.6 Biomimetic scaffolds for 3D cell culture

Design of artificial extracellular matrix (ECM) mimics is one of the major challenges in the development of advanced functional biomaterials. In particular, fabricating simple, inexpensive, robust and reproducible three-dimensional scaffolds that combine all the essential characteristics of the natural ECM, such as the ability to direct and control cell behavior, is an important unmet need. Towards this goal, Ulijn, Gough and co-workers developed a 3D-scaffold for anchorage-dependent cells through biomimetic co-assembly of a minimalistic peptide nanofibrous hydrogel (Fig. 8).51 The ECM-inspired hydrogel scaffold was prepared through a mixture of two aromatic short peptide derivatives, Fmoc-FF (**5**), Fmoc-RGD (**49**) and Fmoc-RGE (**50**) (Fig. 8A). Fmoc-FF can self-assemble into a 3D macroscopic hydrogel nanofiber network and offers a stable structural component to organize the bioactive Fmoc-RGD at the surface of the nanofibers, similar to the peptide orientation in the natural ECM. The co-assembly of the peptide building blocks was probed by various spectroscopy and microscopy techniques which revealed that the intermolecular β-sheets interlocked through π–π stacking of the Fmoc groups, thereby facilitating the formation of a highly hydrated, stiff and cylindrical nanofibrous hydrogel network with the RGDs positioned in tunable densities on the fiber surfaces (Fig. 8B). Furthermore, these rapidly co-assembled hydrogels were successfully applied as 3D scaffolds for promoting the adhesion of encapsulated dermal fibroblasts through specific RGD–integrin binding and subsequent cell spreading and proliferation (Fig. 8C–E). These results suggest the potential of biomimetic short peptide supramolecular co-assembly to study, direct and control cell behavior within a 3D environment, allowing new advances in the field of cell therapy, tissue engineering and fundamental cell biology.

3.7 Fluorescence modulation

Though quite challenging, the ability to integrate and precisely control the composition of multiple biomolecular functional building blocks is essential for many biological applications, in vaccines, tissue engineering, drug delivery and theranostics. In this context, Collier and co-workers demonstrated a simple yet versatile co-assembly route to fabricate multiple fluorescent proteins into a single nanostructure and gel with exceptional compositional and resultant fluorescence color control (Fig. 9).52 The method employs

mixing of non-assembled ‘β-Tail’ tags (**51**) with a β-sheet fibrilizing short peptide (**52**) to induce co-assembly into a one-dimensional molecular organization. This strategy enables the integration of multiple dissimilar β-Tail fusion proteins into peptide nanofibers, alone or in combinations, at predictable and finely tuned concentrations. Furthermore, this method was successfully applied to achieve precisely tailored hues using mixtures of fluorescent proteins, to fabricate nanofibers bearing enzymatic activity, and to adjust antigenic dominance in vaccines.

4 Conclusion and outlook

In summary, minimalistic supramolecular peptide co-assembly is an emerging area of research, paving the way to provide an attractive alternative to time-consuming and inaccessible chemical synthesis. Drawing inspiration from living systems, researchers have successfully achieved well-defined peptide co-assembly modes. The integration of precisely designed multiple functionality peptide building blocks improves the structural complexity and chemical diversity within the co-assembled system and thus increases the conformational space in nanotechnology. The dynamic complex co-assembly pathways enable the formation of non-canonical topologies with tailor-made physical, chemical and mechanical properties. Moreover, this strategy can be effectively employed in a wide spectrum of applications, ranging from the fabrication of devices to the treatment of diseases.

Although significant advancement has been made in the field, the full promise of peptide supramolecular co-assembly has not been fully realized yet. Like natural sequence-specific functional proteins, the effective programmable co-organization of multiple peptide building blocks and thereby coherent modulation of characteristics are an important unmet challenge. The precise order regulation within the peptide co-assemblies can impart remarkable advances in nanotechnology. More emphasis on stimuli responsive co-assembled peptide hydrogels and nanostructures is equally important and constitutes future directions for the development of advanced functional smart nanomaterials. Moreover, the study of supramolecular co-assembly among biologically significant short peptides will shed light on various mysterious noncovalent protein folding physiologies, pathology and drug design. Overall, we believe that the intrinsic simplicity and multifaceted characteristics of minimalistic peptide supramolecular co-assembly provide an important step forward to bridge the gap between biopolymers and peptide self-assembly.

Acknowledgements

This work was partially supported by grants from the Israeli National Nanotechnology Initiative, the Helmsley Charitable Trust for a Focal Technology Area on Nanomedicine for Personalized Theranostics, and the European Research Council under the European Union’s Horizon 2020 research and innovation program (BISON, Advanced ERC grant, no. 694426) (E. G.). P. M. gratefully acknowledges the Center for Nanoscience and Nanotechnology of Tel Aviv University for financial support. The authors thank Kai Tao for his valuable assistance in figure preparation, Sigal Rencus-Lasar for linguistic editing and all the members of the Gazit laboratory for helpful discussions.

Biographies

Pandeeswar Makam Dr. Pandeeswar Makam obtained his PhD degree in 2016 from Jawaharlal Nehru Centre for Advanced Scientific Research (JNCASR), India. Subsequently, he joined the Prof. Ehud Gazit's research group as a postdoctoral fellow under the Center for Nanoscience and Nanotechnology Post-Doctoral Fellowship program, Tel Aviv University. His research interests include bio-inspired minimalistic peptide supramolecular nanoassemblies for optical, electronic and biological applications.

Ehud Gazit Prof. Ehud Gazit is the incumbent Chair for Biotechnology of Neurodegenerative Diseases at Tel Aviv University. He received his BSc (summa cum laude) after completing his studies at the Special University Program for Outstanding Students at Tel Aviv University and his PhD (with highest distinction) from the Weizmann Institute of Science. He has been a faculty member at Tel Aviv University since 2000, following the completion of his postdoctoral studies at Massachusetts Institute of Technology (MIT). He is a member of the European Molecular Biology Organization (EMBO) and a Fellow of the Royal Society of Chemistry (FRSC). In 2015, he was knighted by the Italian Republic for his service to science and society. Prof. Gazit has received numerous awards including the Landau Research Award, the Dan David Scholarship Award, the Herstin Award for a leading scientist under the age of 44 in 2009, the Research Prize Award named after Teva Founders in 2013, and the Kadar Family Award in 2015.

References

1. Lehn J-M. Science. 1993; 260:1762–1763. [PubMed: 8511582]
2. Whitesides GM. Science. 2002; 295:2418–2421. [PubMed: 11923529]
3. Aida T, Meijer EW, Stupp SI. Science. 2012; 335:813–817. [PubMed: 22344437]
4. Philp D, Stoddart JF. Angew Chem, Int Ed Engl. 1996; 35:1154–1196.
5. Tao K, Makam P, Aizen R, Gazit E. Science. 2017; 358:eaam9756. [PubMed: 29146781]
6. Zhang S. Nat Biotechnol. 2003; 21:1171–1178. [PubMed: 14520402]
7. Webber MJ, Appel EA, Meijer EW, Langer R. Nat Mater. 2015; 15:13–26.
8. Reches M, Gazit E. Science. 2003; 300:625–627. [PubMed: 12714741]

9. Adler-Abramovich L, Aronov D, Beker P, Yevnin M, Stempler S, Buzhansky L, Rosenman G, Gazit E. Nat Nanotechnol. 2009; 4:849–854. [PubMed: 19893524]
10. Reches M, Gazit E. Nat Nanotechnol. 2006; 1:195–200. [PubMed: 18654186]
11. Berger O, Adler-Abramovich L, Levy-Sakin M, Grunwald A, Liebes-Peer Y, Bachar M, Buzhansky L, Mossou E, Forsyth VT, Schwartz T, Ebenstein Y, et al. Nat Nanotechnol. 2015; 10:353–360. [PubMed: 25775151]
12. Gazit E. Chem Soc Rev. 2007; 36:1263. [PubMed: 17619686]
13. Frederix PWJM, Scott GG, Abul-Haija YM, Kalafatovic D, Pappas CG, Javid N, Hunt NT, Ulijn RV, Tuttle T. Nat Chem. 2014; 7:30–37. [PubMed: 25515887]
14. Arnon ZA, Vitalis A, Levin A, Michaels TCT, Caflisch A, Knowles TPJ, Adler-Abramovich L, Gazit E. Nat Commun. 2016; 7:13190. [PubMed: 27779182]
15. Adler-Abramovich L, Gazit E. Chem Soc Rev. 2014; 43:6881–6893. [PubMed: 25099656]
16. Yan X, Zhu P, Li J. Chem Soc Rev. 2010; 39:1877. [PubMed: 20502791]
17. Fleming S, Ulijn RV. Chem Soc Rev. 2014; 43:8150–8177. [PubMed: 25199102]
18. Fleming S, Debnath S, Frederix PWJM, Hunt NT, Ulijn RV. Biomacromolecules. 2014; 15:1171–1184. [PubMed: 24568678]
19. Liyanage W, Vats K, Rajbhandary A, Benoit DSW, Nilsson BL. Chem Commun. 2015; 51:11260–11263.
20. Pandeeswar M, Senanayak SP, Narayan KS, Govindaraju T. J Am Chem Soc. 2016; 138:8259–8268. [PubMed: 27305598]
21. Adler-Abramovich L, Marco P, Arnon ZA, Creasey RCG, Michaels TCT, Levin A, Scurr DJ, Roberts CJ, Knowles TPJ, Tendler SJB, Gazit E. ACS Nano. 2016; 10:7436–7442. [PubMed: 27351519]
22. Ryan DM, Doran TM, Nilsson BL. Langmuir. 2011; 27:11145–11156. [PubMed: 21815693]
23. Hsu S-M, Wu F-Y, Lai T-S, Lin Y-C, Lin H-C. RSC Adv. 2015; 5:22943–22946.
24. Halperin-Sternfeld M, Ghosh M, Sevostianov R, Grigoriants I, Adler-Abramovich L. Chem Commun. 2017; 53:9586–9589.
25. Li S, Mehta AK, Sidorov AN, Orlando TM, Jiang Z, Anthony NR, Lynn DG. J Am Chem Soc. 2016; 138:3579–3586. [PubMed: 26942690]
26. Behanna, Ha; Rajangam, K; Stupp, SI. J Am Chem Soc. 2007; 129:321–327. [PubMed: 17212411]
27. Behanna HA, Donners JJJM, Gordon AC, Stupp SI. J Am Chem Soc. 2005; 127:1193–1200. [PubMed: 15669858]
28. Swanekamp RJ, DiMaio JTM, Bowerman CJ, Nilsson BL. J Am Chem Soc. 2012; 134:5556–5559. [PubMed: 22420540]
29. Nagy KJ, Giano MC, Jin A, Pochan DJ, Schneider JP. J Am Chem Soc. 2011; 133:14975–14977. [PubMed: 21863803]
30. Morris KL, Chen L, Raeburn J, Sellick OR, Cotanda P, Paul A, Griffiths PC, King SM, O'Reilly RK, Serpell LC, Adams DJ. Nat Commun. 2013; 4:1480. [PubMed: 23403581]
31. Raeburn J, Alston B, Kroeger J, McDonald TO, Howse JR, Cameron PJ, Adams DJ. Mater Horiz. 2014; 1:241–246.
32. Abul-Haija YM, Roy S, Frederix PWJM, Javid N, Jayawarna V, Ulijn RV. Small. 2014; 10:973–979. [PubMed: 24027125]
33. Cinar G, Ozdemir A, Hamsici S, Gunay G, Dana A, Tekinay AB, Guler MO. Biomater Sci. 2017; 5:67–76.
34. Ustun Yaylaci S, Sardan Ekiz M, Arslan E, Can N, Kilic E, Ozkan H, Orujalipoor I, Ide S, Tekinay AB, Guler MO. Biomacromolecules. 2016; 17:679–689. [PubMed: 26716910]
35. Nagy-Smith K, Beltramo PJ, Moore E, Tycko R, Furst EM, Schneider JP. ACS Cent Sci. 2017; 3:586–597. [PubMed: 28691070]
36. Swanekamp RJ, Welch JJ, Nilsson BL. Chem Commun. 2014; 50:10133–10136.
37. Creasey RCG, Louzao I, Arnon ZA, Marco P, Adler-Abramovich L, Roberts CJ, Gazit E, Tendler SJB. Soft Matter. 2016; 12:9451–9457. [PubMed: 27841428]
38. Yuran S, Razvag Y, Reches M. ACS Nano. 2012; 6:9559–9566. [PubMed: 23061818]

39. Maity S, Nir S, Reches M. J Mater Chem B. 2014; 2:2583.
40. Guo C, Arnon ZA, Qi R, Zhang Q, Adler-Abramovich L, Gazit E, Wei G. ACS Nano. 2016; 10:8316–8324. [PubMed: 27548765]
41. Li J, Du X, Hashim S, Shy A, Xu B. J Am Chem Soc. 2017; 139:71–74. [PubMed: 27997165]
42. Channon KJ, Devlin GL, MacPhee CE. J Am Chem Soc. 2009; 131:12520–12521. [PubMed: 19678637]
43. Chen L, Revel S, Morris K, Adams DJ. Chem Commun. 2010; 46:4267.
44. Ardoña HAM, Tovar JD. Chem Sci. 2015; 6:1474–1484. [PubMed: 29560236]
45. Ardoña HAM, Draper ER, Citossi F, Wallace M, Serpell LC, Adams DJ, Tovar JD. J Am Chem Soc. 2017; 139:8685–8692. [PubMed: 28578581]
46. Khalily MA, Bakan G, Kucukoz B, Topal AE, Karatay A, Yaglioglu HG, Dana A, Guler MO. ACS Nano. 2017; 11:6881–6892. [PubMed: 28679051]
47. López-Andarias J, Rodriguez MJ, Atienza C, López JL, Mikie T, Casado S, Seki S, Carrascosa JL, Martín N. J Am Chem Soc. 2015; 137:893–897. [PubMed: 25530351]
48. Nalluri SKM, Shivarova N, Kanibolotsky AL, Zelzer M, Gupta S, Frederix PWJM, Skabara PJ, Gleskova H, Ulijn RV. Langmuir. 2014; 30:12429–12437. [PubMed: 25259412]
49. Huang Z, Guan S, Wang Y, Shi G, Cao L, Gao Y, Dong Z, Xu J, Luo Q, Liu J. J Mater Chem B. 2013; 1:2297.
50. Wang M, Lv Y, Liu X, Qi W, Su R, He Z. ACS Appl Mater Interfaces. 2016; 8:14133–14141. [PubMed: 27191381]
51. Zhou M, Smith AM, Das AK, Hodson NW, Collins RF, Ulijn RV, Gough JE. Biomaterials. 2009; 30:2523–2530. [PubMed: 19201459]
52. Hudalla GA, Sun T, Gasiorowski JZ, Han H, Tian YF, Chong S, Collier JH. Nat Mater. 2014; 13:829–836. [PubMed: 24930032]

Europe PMC Funders Author Manuscripts

Europe PMC Funders Author Manuscripts

Key learning points

(1) The interplay between covalent co-polymer chemistry and minimalistic supramolecular peptide co-assembly

(2) Types of peptide co-assembly processes and the resulting structures

(3) Key strategies to promote peptide co-assembly

(4) The technological applications of peptide co-assembly

Europe PMC Funders Author Manuscripts

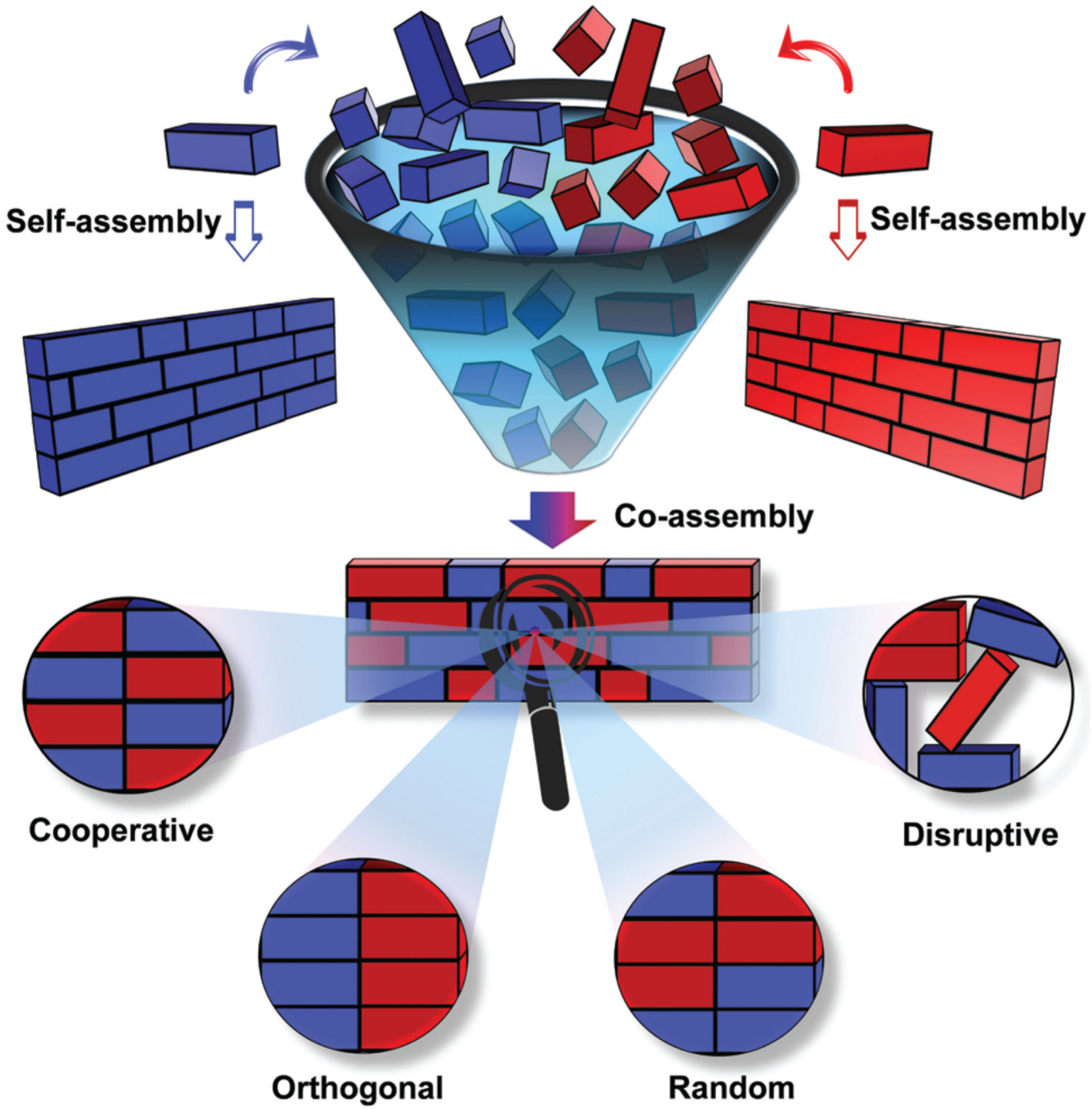

Fig. 1.

Peptide supramolecular co-polymers. Schematic illustration of how two peptide building blocks (blue and red bricks) can self-assemble into an ordered architecture (blue or red wall); mixing them results in a complex co-assembled architecture (wall comprises both blue and red bricks) *via* four possible supramolecular co-polymer arrangements such as cooperative, orthogonal (or self-sorting), random and disruptive co-assembly.

Europe PMC Funders Author Manuscripts

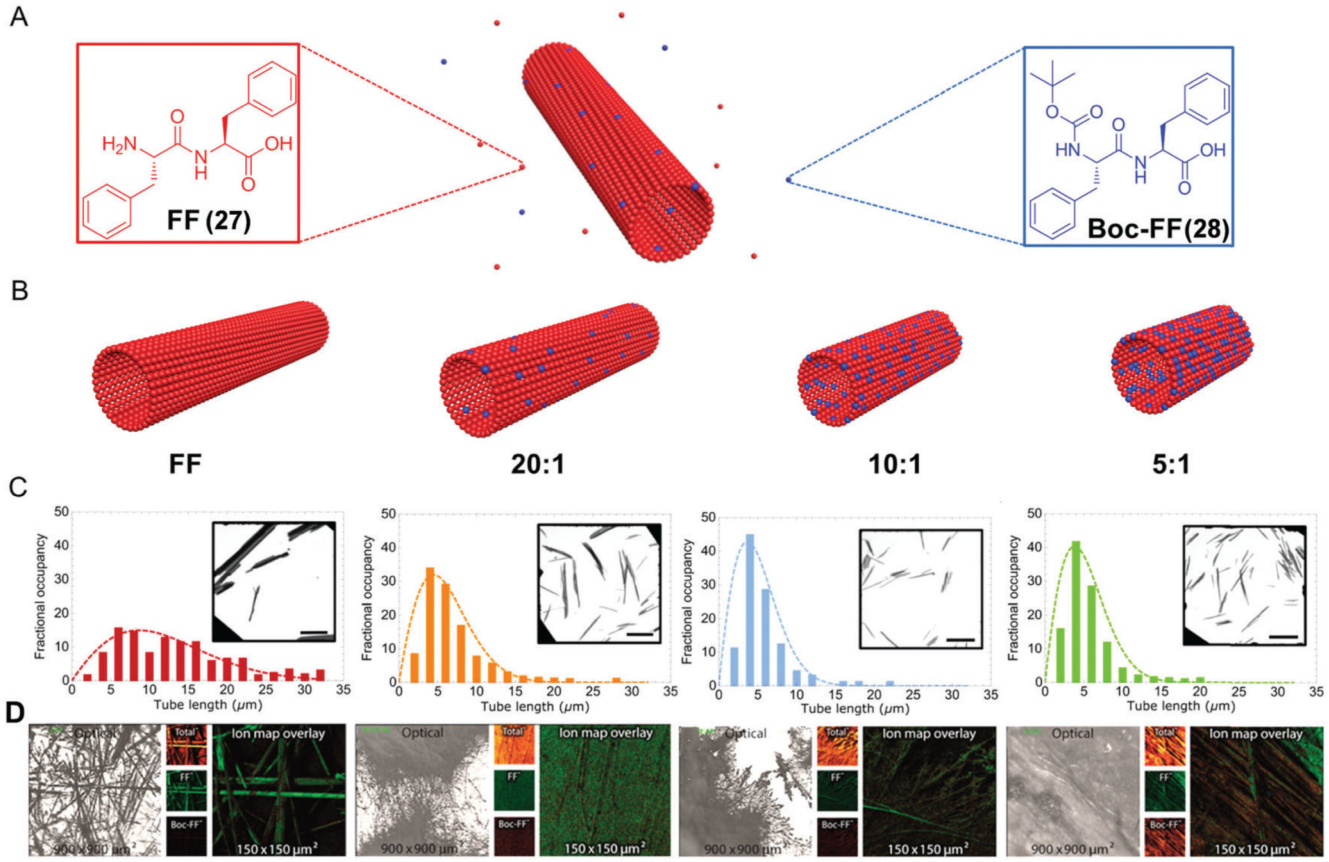

Fig. 2.

Peptide supramolecular co-assembly driven dimensional control. (A and B) Chemical structures and schematic illustration of FF nanotube physical dimensional control *via* co-assembly with Boc-FF at the different molar ratios. (C and D) The corresponding histograms of the nanotube length distributions (μm) (insets: transmission electron microscopy images, scale bar 10 μm) and ToF-SIMS analysis (optical micrograph (left), ToF-SIMS chemical maps (right)) respectively. Reproduced with permission from ref. 21 Copyright 2016, American Chemical Society.

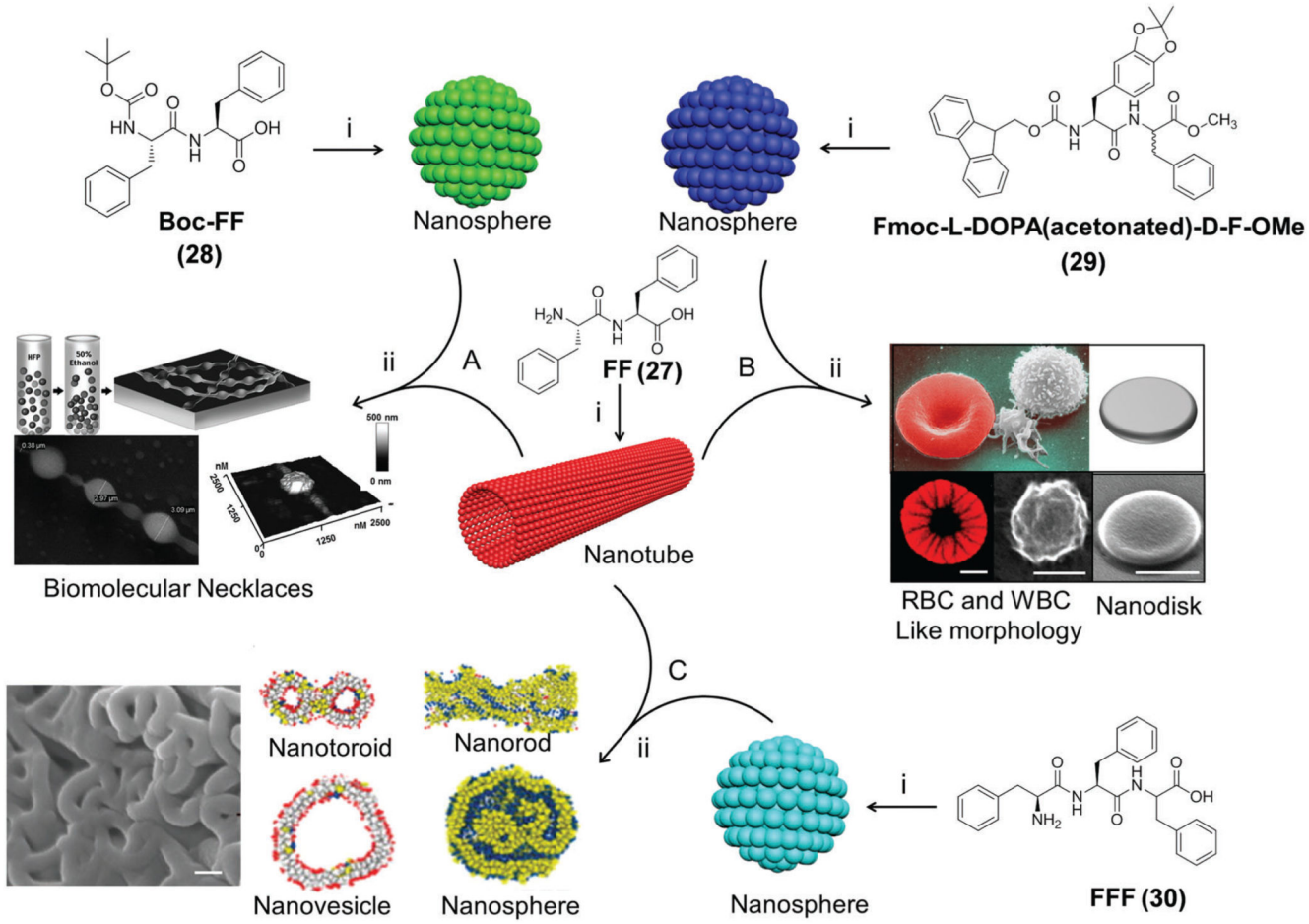

Fig. 3.

Creation of non-canonical complex peptide topologies *via* supramolecular co-assembly. (A) Co-assembly of FF and Boc-FF into a biomolecular necklace like architecture; scanning electron microscopy (SEM) and 3D atomic force microscopy (AFM) image of co-assembled necklaces (reproduced with permission from ref. 38 Copyright 2012, American Chemical Society). (B) Co-assembly of FF with Fmoc-(L)DOPA(acetonated)-(D)F-OMe into red (RBC) and white (WBC) blood cell-like and disk-like nanostructures, fluorescence (doxorubicin adsorbed) and SEM images, scale bar 1 μm (reproduced with permission from ref. 39 Copyright 2014, Royal Society of Chemistry). (C) Co-assembly of FF with FFF to form diverse molar ratio dependent tunable nanomorphologies including nanotoroids, nanovesicles, nanorods, and nanospheres; SEM image of a nanotoroid, scale bar 100 nm (reproduced with permission from ref. 40 Copyright 2016, American Chemical Society). (i) Self-assembly; (ii) co-assembly process.

Europe PMC Funders Author Manuscripts

Europe PMC Funders Author Manuscripts

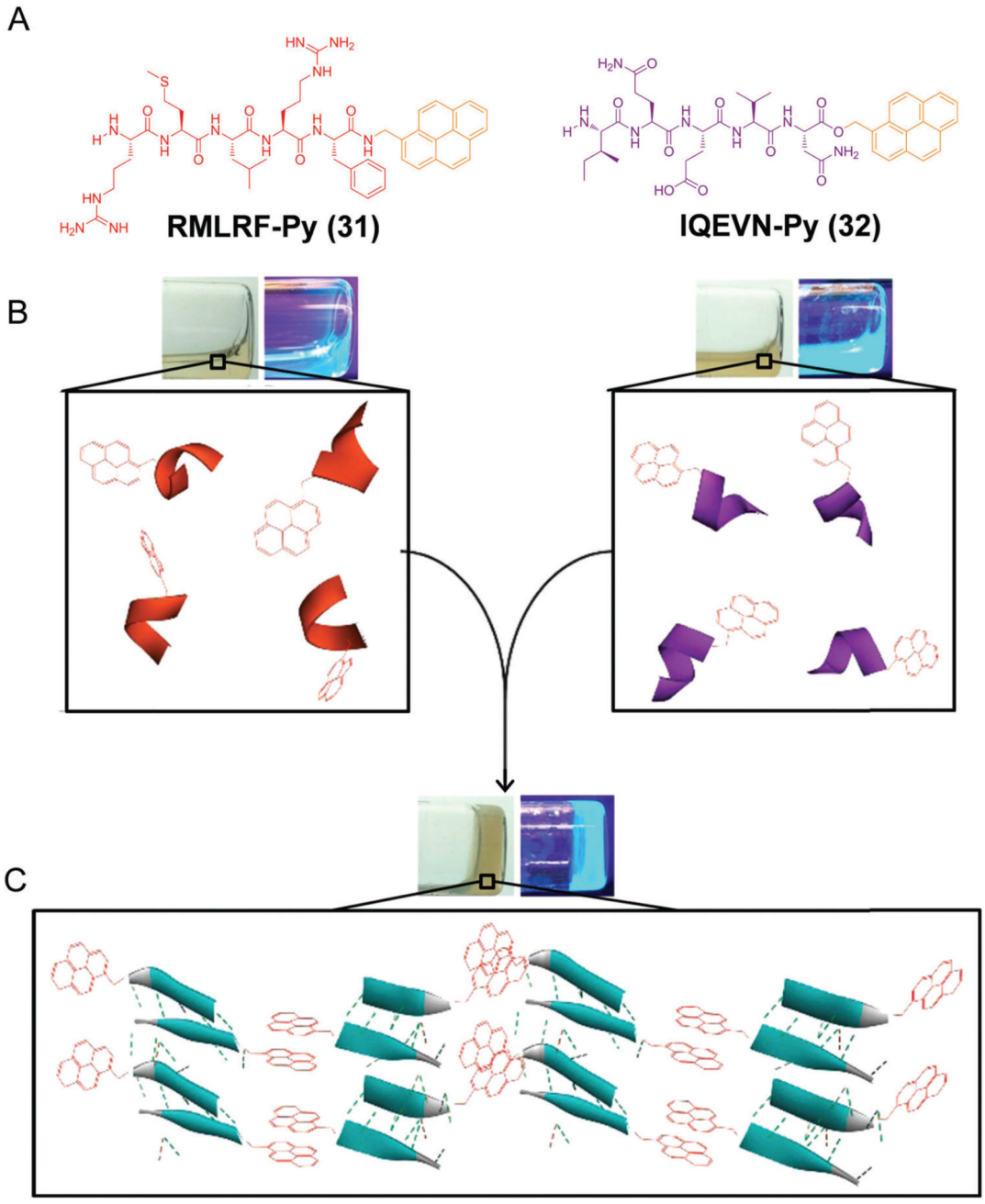

Fig. 4.

Co-assembly driven peptide secondary structural transition. (A) Chemical structures of pyrene conjugated peptides. (B) Solutions (under visible and UV light) of individual peptide conjugates comprising an α-helix like conformation. (C) Supramolecular co-assembly driven hydrogels comprising a β-sheet-like conformation. Reproduced with permission from ref. 41 Copyright 2017, American Chemical Society.

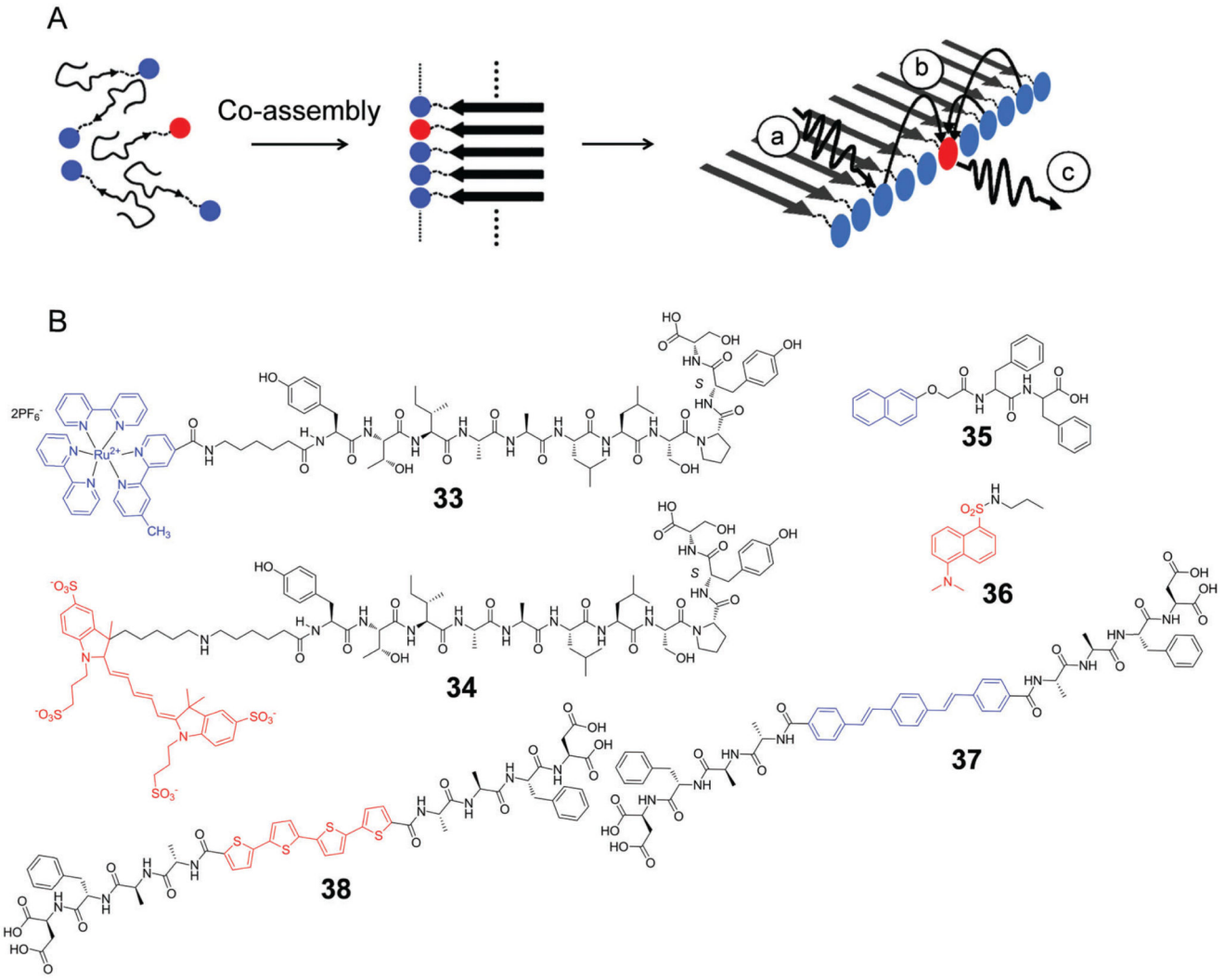

Fig. 5.

Light harvesting peptide supramolecular co-assemblies. (A) Schematic illustration of the organic fluorophore (donors (blue disk) and acceptors (red disks)) conjugated peptide component (arrow). Supramolecular co-assembly driven donor–acceptor light harvesting system *via* (a) absorption of a photon by the donor, (b) nonradiative transfer to an acceptor *via* resonance energy transfer (RET) and (c) the release of energy from the acceptor (reproduced with permission from ref. 42 Copyright 2009, American Chemical Society). (B) Chemical structures of donor and acceptor peptide conjugate pairs (**33**/**34**; **35**/**36** and **37**/**38**).

Europe PMC Funders Author Manuscripts

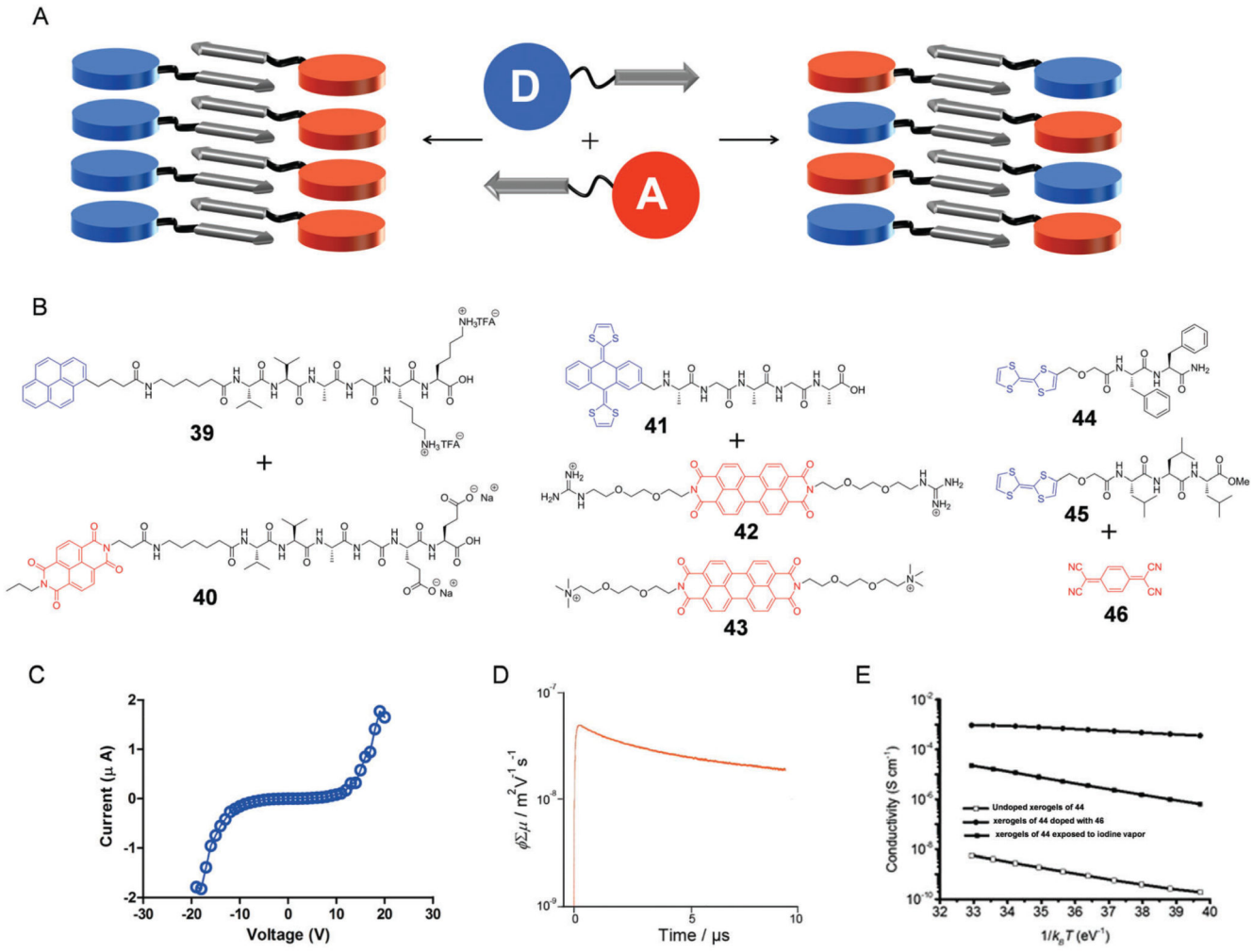

Fig. 6.

Electrically conducting peptide supramolecular co-assemblies. (A) Schematic illustration of the organic aromatic chromophore (donors (blue disk) and acceptors (red disks)) conjugated peptide component (arrow) and its possible co-assembly organization. (B) Chemical structures of donor and acceptor peptide conjugate pairs (**39/40**; **41/42**, **41/43**, **44/46** and **45/46**). (C) Current–voltage (*I–V*) characteristics of the **39/40** co-assembled film (reproduced with permission from ref. 46 Copyright 2017, American Chemical Society). (D) Conductivity transients observed for **41/42** upon exposure at 355 nm, 9.1 x 10^{15} photons per cm^2 (reproduced with permission from ref. 47 Copyright 2015, American Chemical Society). (E) The temperature-dependent conductivity measurements of the **44** xerogels before and after co-assembly or doping (reproduced with permission from ref. 48 Copyright 2014, American Chemical Society).

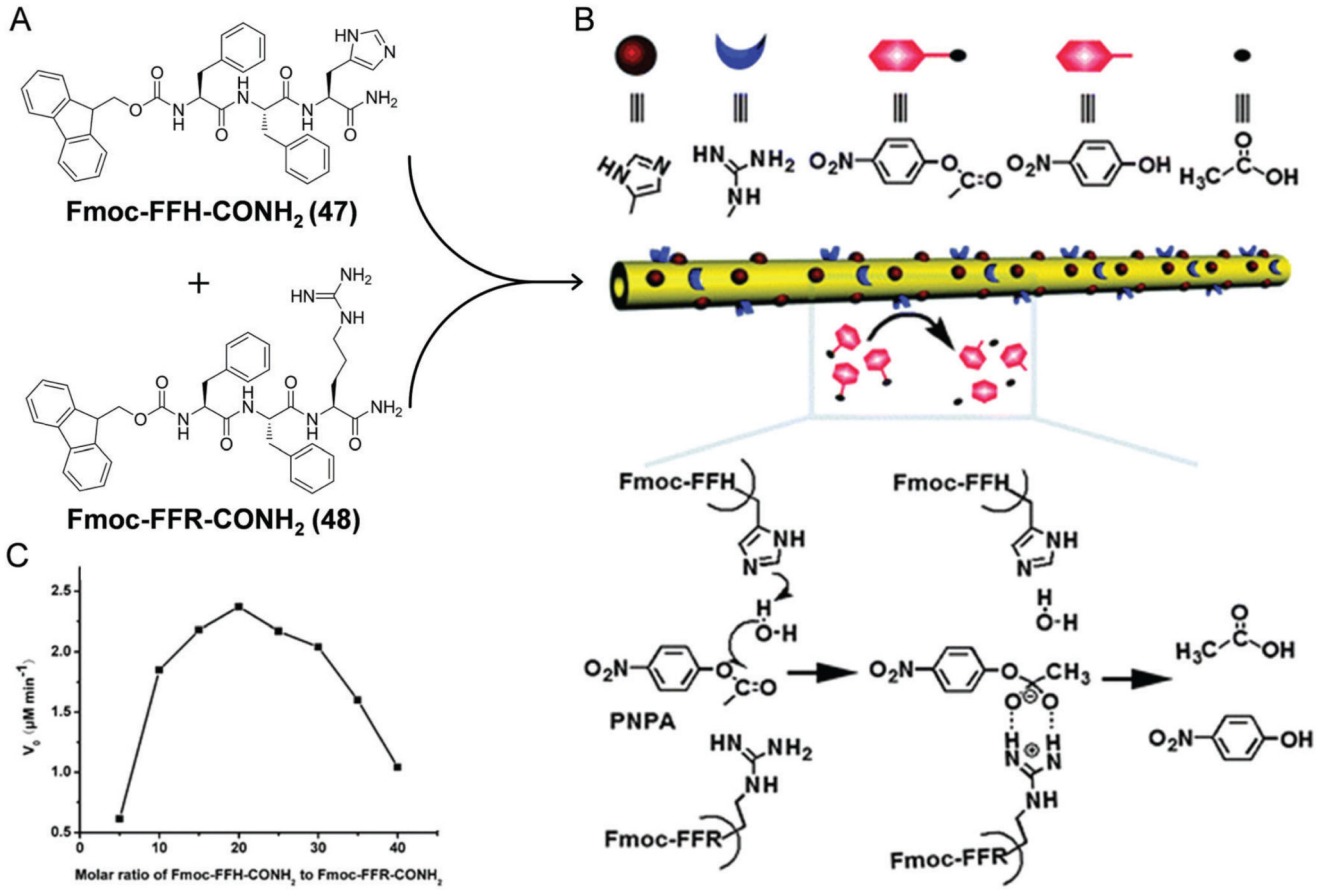

Fig. 7.

Biocatalytic supramolecular peptide co-assembly. (A) Molecular structures of peptide amphiphiles. (B) Schematic representation of the coassembly of **47** and **48** into nanotubes with catalytically active functionalities (imidazolyl and guanidyl) and on the surface and possible mechanism for the *p*-NPA hydrolysis. (C) The plot of catalytic reaction rate *vs.* molar ratio of Fmoc-FFH-$CONH_2$ to Fmoc-FFR-$CONH_2$. Reproduced with permission from ref. 49 Copyright 2013, Royal Society of Chemistry.

Europe PMC Funders Author Manuscripts

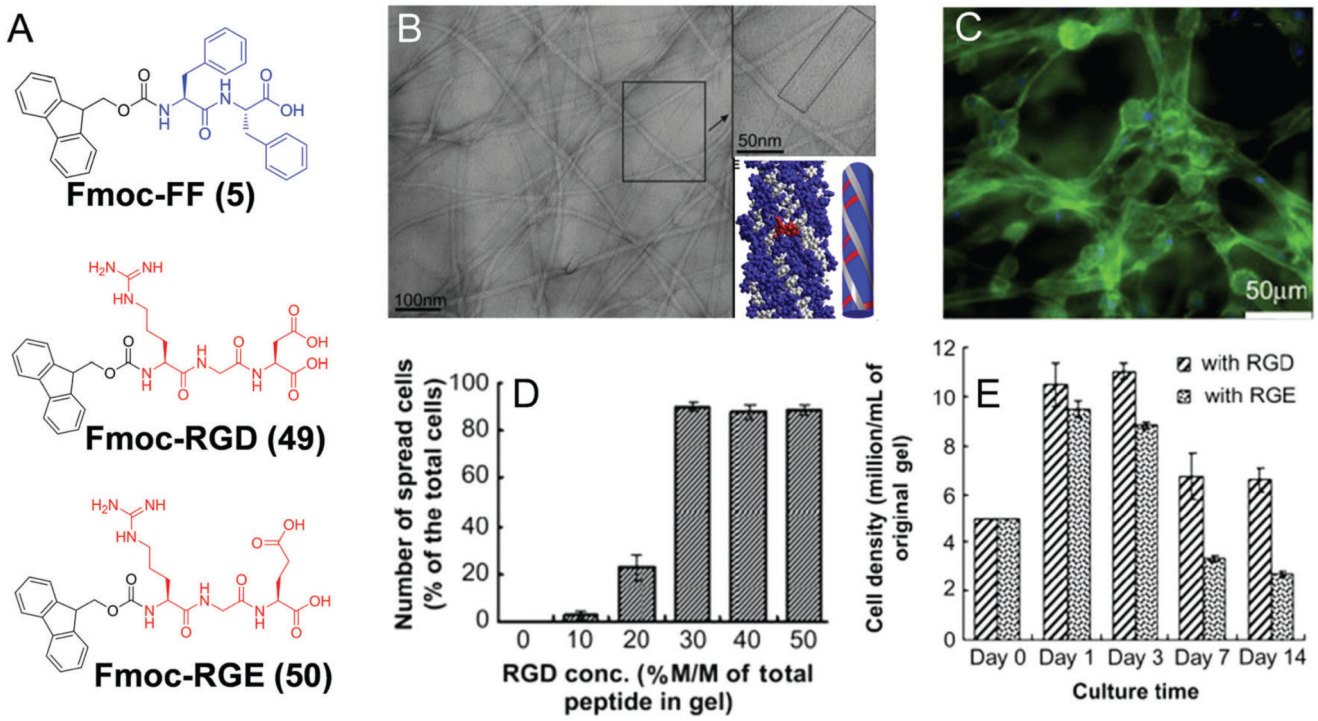

Fig. 8.

Peptide supramolecular co-assemblies as scaffolds for 3D cell culture. (A) Chemical structures of peptide amphiphiles. (B) TEM images of Fmoc-FF/RGD co-assembled nanofibers and the proposed supramolecular co-assembly model. (C) Human adult dermal fibroblast (HDFa) adhesion and morphology in the Fmoc-FF/RGD hydrogels 48 h post culture. (D) Influence of Fmoc-RGD/FF concentration ratio on cell spreading. (E) Cell proliferation in the Fmoc-FF/RGD and Fmoc-FF/RGE hydrogels. Reproduced with permission from ref. 51 Copyright 2009, Elsevier.

Europe PMC Funders Author Manuscripts

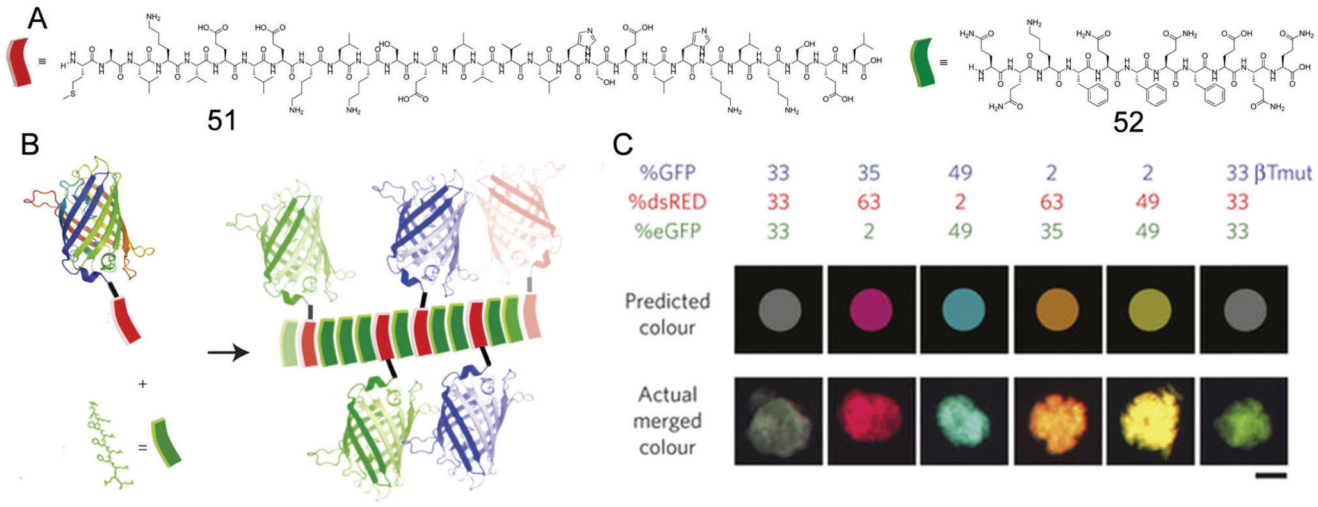

Fig. 9.

Peptide supramolecular co-assembly driven fluorescence modulation. (A) Chemical structures of the β-sheet fibrillizing fusion domain and β-sheet fibrillizing peptide. (B) Schematic representation of co-assembly between fusion fluorescent proteins having a β-sheet fibrillizing domain and β-sheet fibrillizing peptides to form nanofibres with a precise combination of protein ligands. (C) Different fluorescent β-Tail proteins co-assembled into microgels at a precisely tunable dose, demonstrating close correlation between the actual gel color and the predicted color, scale bar 40 μm. Reproduced with permission from ref. 52 Copyright 2014, Nature Publishing Group.

Europe PMC Funders Author Manuscripts

Table 1

The design strategies for making minimalistic peptide supramolecular co-assemblies

Method	Peptide	Ref.
Aromatic interactions	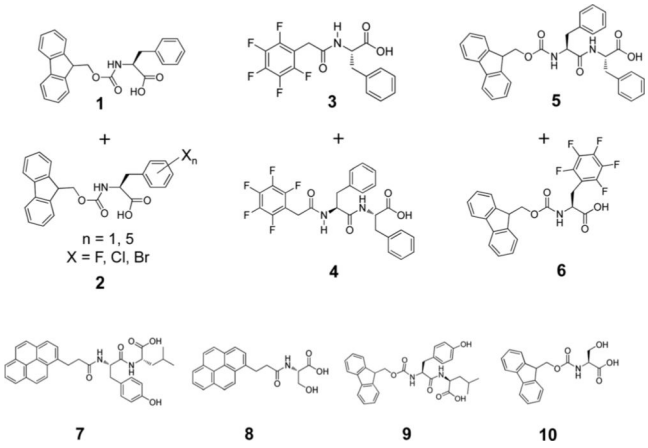	18 and 22–24
Electrostatic interactions	Ac-KLVFFAL-NH_2 (**11**) + Ac-(pY)VFFAL-NH_2 (**12**) $C_{15}H_{31}$CONH-V-V-V-A-A-A-E-E-E-COOH (**13**) + Asp($CONHC_{12}$)-V-V-V-V-V-V-K-K-K-NH_2 (**14**)	25 and 27
Enantiomeric peptide	VKVKVKVKV^{D}P^{L}PTKVKVKVKV-NH_2 (**15**) + VKVKVKVKV^{L}P^{D}PTKVKVKVKV-NH_2 (**16**) L-Ac-$(FKFE)_2$-NH_2 (**17**) + D-Ac-$(FKFE)_2$-NH_2 (**18**)	28 and 29
Chemical stimuli	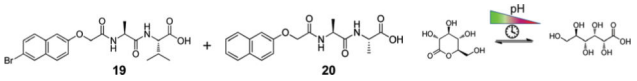	30
Electrochemical stimuli	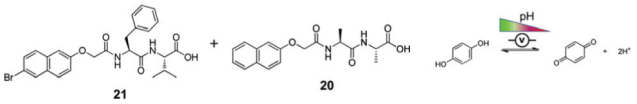	31
Enzymatic action	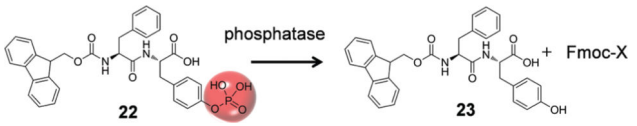 Fmoc-X = Fmoc-S (**24**), Fmoc-T (**25**) and Fmoc-RGD (**26**)	32